# An Investigation of Photocurrent Generation by Gold Electrodes Modified with Self-Assembled Monolayers of $C_{60}$

**Hiroshi Imahori,* Takayuki Azuma, Anawat Ajavakom, Hiroyuki Norieda, Hiroko Yamada, and Yoshiteru Sakata***

*The Institute of Scientific and Industrial Research, Osaka University, Mihoga-oka, Ibaraki, Osaka 567-0047, Japan*

*Received: March 9, 1999; In Final Form: May 18, 1999*

Three different kinds of $C_{60}$ alkanethiols have been prepared by changing systematically the linking positions, ortho, meta, and para, at a phenyl group on a pyrolidine ring fused to the $C_{60}$ moiety. Electrochemical measurements showed that well-ordered structures are formed in self-assembled monolayers of these $C_{60}$ alkanethiols on gold electrodes. Photoelectrochemical studies were carried out using gold electrodes modified with self-assembled monolayers of the $C_{60}$. A stable anodic photocurrent was observed in the presence of an electron sacrificer when the modified gold electrode was illuminated with a monochromic light. Dependence of the photocurrents on the applied potential together with the agreement of the action spectra with the absorption spectra support the following photocurrent generation mechanism: the generation of a vectorial electron flow from the electron sacrificer to the gold electrode via the excited triplet state of the $C_{60}$. The quantum yields vary from 7.5% to 9.8%, depending on the linking positions.

Since their discovery, fullerenes have continuously attracted much interest from many researchers, because of the unique three-dimensional structures with delocalized $\pi$ electrons.[1] In particular, fullerene thin films formed using a variety of methods such as Langmuir−Blodgett (LB) techniques and evaporation have exhibited interesting electrochemical, photochemical, and optical properties.[2] However, these physisorbed fullerene films lack the stability and uniformity at the nanoscale level. Self-assembled monolayers (SAMs) are a promising method for constructing highly ordered, densely packed structures on substrates.[3] Thus, well-ordered, two-dimensional monolayers of fullerenes will be obtained when they are attached to the terminal group of SAMs. So far there have been several reports of $C_{60}$ SAMs.[4−11] These include preparation, electrochemistry, and structural characterization using atomic force microscopy. Recently we have reported the preliminary photoelectrochemical properties of a SAM of $C_{60}$ on a gold electrode.[12] The high quantum yield (7.5%) of the $C_{60}$ cell prompted us to investigate the photoelectrochemical properties in details. Here we report the preparation, electrochemistry, and photoelectrochemistry of SAMs of $C_{60}$-tethered alkanethiols **1** on gold electrodes (Figure 1).

It is well established that alkanethiols with a polymethylene chain ((number of the methylenes) ≥ 10) form densely packed monolayers on gold surfaces. The presence of an amido group in a chain enhances the stability of monolayers as a result of the intermolecular hydrogen bonding.[13−17] Thus, it is expected that the attachment of a long alkyl chain including an amide linkage to $C_{60}$ would allow us to produce a well-ordered, robust structure of the $C_{60}$ SAM on a gold electrode. To explore the relationship between the structure and the photoelectrochemical properties of the monolayers, we employed three different kinds of $C_{60}$ alkanethiols **1** where the linking position is varied systematically from ortho to para at the phenyl group on the pyrolidine ring fused to the $C_{60}$ moiety. The underlying rigid saturated hydrocarbon backbones will make it possible to evaluate the linkage dependence upon photoelectrochemistry in the $C_{60}$ SAMs on gold electrodes.

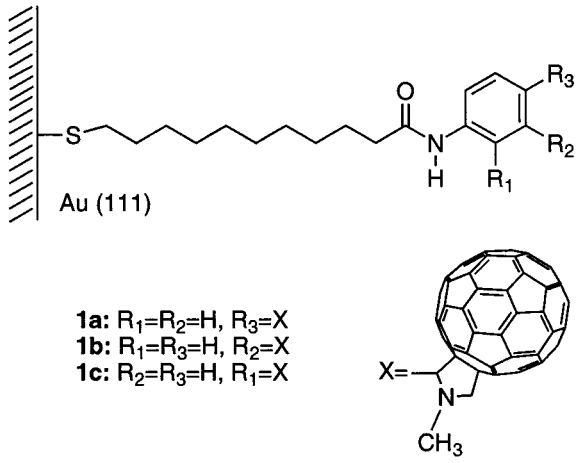


**Figure 1.** Self-assembled monolayers of **1** on gold electrodes.

## Experimental Section

**Materials and Preparation.** Synthesis and characterization of **1** are described in Supporting Information. An attempt to synthesize $C_{60}$ thiols with shorter linkages was unsuccessful because of the poor solubility. Gold electrodes were prepared by a vacuum deposition technique with chromium (50 Å) and gold (2000 Å) in a sequence onto a Si (100) wafer (Sumitomo Sitix Corp.). Atomic force microscopy (Seiko Instruments) and X-ray diffraction studies showed that the gold electrodes have mainly Au(111) surfaces. The roughness factor (1.1) was estimated by iodine chemisorption on the Au(111) surface. The gold-coated wafers were cut into slides (ca. 1−3 cm × 1−3 cm), rinsed with dilute hydrochloric acid, Millipore water, and

* Corresponding authors. E-mail: imahori@sanken.osaka-u.ac.jp; sakata@sanken.osaka-u.ac.jp. Fax: 81-6-6879-8479.

10.1021/jp990837k CCC: $18.00 
Published on Web 08/10/1999

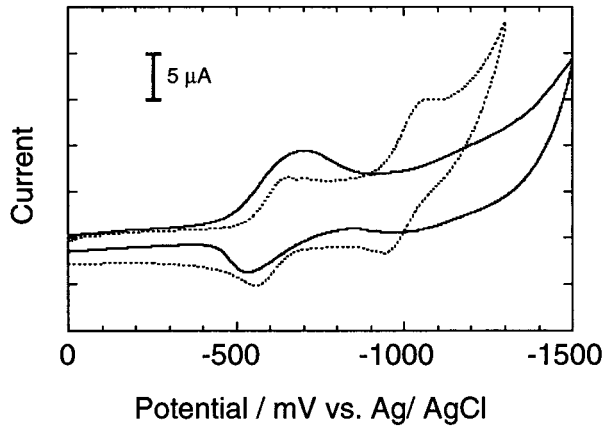


**Figure 2.** Cyclic voltammograms of **1a** in $CH_2Cl_2$ (dotted line) and **1a**/Au in $CH_2Cl_2$ (solid line): sweep rate 100 mV $s^{-1}$, electrode area 0.48 $cm^2$, initial potential 0 V.

ethanol, and dried with a stream of argon before being immersed in a solution of thiols. Monolayers were formed by the spontaneous adsorption of the thiols onto the gold substrates. In all cases, adsorption was carried out from $CHCl_3$ solutions of $2.0 \times 10^{-5}$ M at 25 °C for 20 h to reach the equilibrium. After soaking, the electrode was washed well with $CHCl_3$ and dried with a stream of argon. Reliable absorption spectra of **1** on gold electrode could not be obtained in reflection or transmission modes because of the low absorbance of the $C_{60}$.

**Electrochemical and Photoelectrochemical Measurements.** All electrochemical studies were performed on a Bioanalytical Systems, Inc. CV-50W voltammetric analyzer using a standard three-electrode cell with a modified Au working electrode (0.48 $cm^2$), platinum wire counter electrode, and a Ag/AgCl (saturated KCl) reference. Photoelectrochemical measurements were performed in a one-compartment Pyrex UV cell (5 mL) under argon atmosphere. The cell was illuminated with monochromatic excitation light through interference filters (MIF−S, Vacuum Optics Corporation of Japan) by a 180 W UV lamp (Sumida LS-140UV) on the SAM of 0.48 $cm^2$. Unless otherwise stated, a 0.1 M $Na_2SO_4$ and $5 \times 10^{-2}$ M ascorbic acid aqueous electrolyte solution (pH 7.0) was used. The photocurrent was measured in a three-electrode arrangement, a modified Au working electrode, platinum wire counter electrode (the distance between the electrodes is 0.3 mm), and Ag/AgCl (saturated KCl) reference. The light intensity was monitored by an Anritsu ML9002A optical power meter.

## Results

**Electrochemistry of $C_{60}$ SAMs.** Figure 2 shows cyclic voltammograms of **1a** in $CH_2Cl_2$ and **1a** on a gold electrode (hereafter, **1a**/Au, where / represents an interface). Cyclic voltammetry of **1a** in $CH_2Cl_2$ containing 0.1 M *n*-$Bu_4NPF_6$ as an electrolyte with a sweep rate of 100 mV $s^{-1}$ exhibited reversible waves as a result of the first and the second reductions of the $C_{60}$ (−0.60, −1.02 V vs Ag/AgCl), which are typical for the monofunctionalized $C_{60}$.[18−22] Similarly, the two successive, reversible waves were seen for **1b** and **1c**. The results are summarized in Table 1.

Cyclic voltammetry of **1a**/Au in $CH_2Cl_2$ containing 0.1 M *n*-$Bu_4NPF_6$ with a sweep rate of 100 mV $s^{-1}$ showed a broad wave at $E_{1/2} = -0.61$ V (vs Ag/AgCl), which corresponds to the first reduction/reoxidation of the $C_{60}$ (Figure 2). The value of the peak splitting ($\Delta E_{peak} = 180$ mV) is large, compared with the ideal value in solution, indicating the slow kinetics between the $C_{60}$ and the gold electrode because of the structural

**TABLE 1: Redox Potentials, Surface Coverage, and Quantum Yields**

| | $E_{1/2}$/V ($\Delta E_{peak}$/V) | | | | |
|---|---|---|---|---|---|
| | soln in $CH_2Cl_2$ | | SAMs[a] | surface coverage, $\Gamma$ /$10^{-10}$ mol $cm^{-2}$ | quantum |
| Thiols | 0/1− | 1−/2− | 0/1− | ($Å^2$ $molecule^{-1}$) | yield /% |
| **1a** | −0.60 | −1.02 | −0.61 (0.18)[b] | 1.4 (120) | 9.8 |
| **1b** | −0.61 | −1.02 | −0.62 (0.18)[b] | 1.3 (130) | 8.6 |
| **1c** | −0.59 | −1.00 | −0.63 (0.21)[b] | 1.4 (120) | 7.5 |

[a] It was difficult to determine the $E_{1/2}$ of the second reduction due to the $C_{60}$ because of the extensive broadening of the waves. [b]Numbers in parentheses indicate the values of the peak separation ($\Delta E_{peak}$/V).

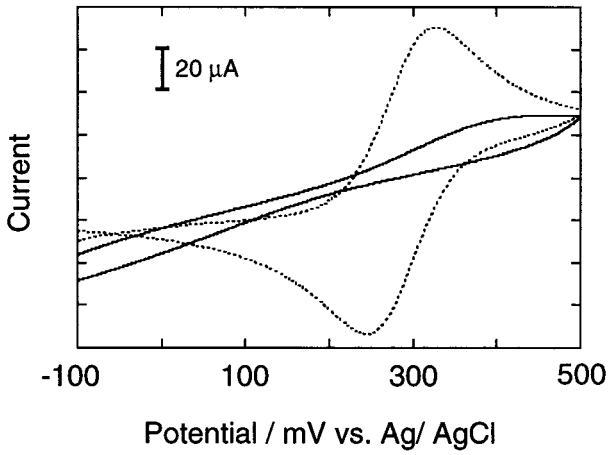


**Figure 3.** Cyclic voltammograms of bare Au (dotted line) and **1a**/Au (solid line) in the presence of 1 mM $K_3[Fe(CN)_6]$: sweep rate 100 mV $s^{-1}$, electrode area 0.48 $cm^2$, initial potential 0 V.

constraint. In contrast, the second wave due to the second reduction/reoxidation of the $C_{60}$ was essentially invisible. Similar results were obtained for **1b**/Au and **1c**/Au. The electrochemical behavior is quite close to that of the previously reported $C_{60}$ SAMs.[4,6,8] Integration of the area under the curve of **1a**/Au observed for the first reduction due to the $C_{60}$ corresponds to a surface coverage of $\Gamma = 1.4 \times 10^{-10}$ mol $cm^{-2}$ (120 $Å^2$ $molecule^{-1}$). The $\Gamma$ values of **1a**−**c**/Au are almost the same (Table 1) and agree well with that ($1.4 \times 10^{-10}$ mol $cm^{-2}$) of the similar $C_{60}$ SAM systems.[8,9] The occupied areas per molecule are somewhat larger than that of the hexagonal (78 $Å^2$ $molecule^{-1}$) or the simple square (98−100 $Å^2$ $molecule^{-1}$) packing in similar $C_{60}$ LB films.[23−25] This may be related to the steric hindrance around the phenyl group on the pyrolidine ring attached to the $C_{60}$.

Figure 3 displays the cyclic voltammetric current−potential ($i-E$) responses for a bare gold electrode and **1a**/Au with 1 mM $Fe(CN)_6^{3-}$ as the electroactive species and 1.0 M $Na_2SO_4$ as an electrolyte.[26] There is a dramatic difference between the $i-E$ responses for the bare gold and monolayer-covered electrodes. A reversible cyclic voltammogram of the redox probe was observed in the former, implying that the redox probe exhibits electrical communication with the bare gold electrode. In contrast, such communication decreases in the latter and becomes irreversible. Similar blocking behavior was observed for **1b**/ Au and **1c**/Au. These data clearly show that the redox communication of $Fe(CN)_6^{3-}$ is interfered by the $C_{60}$ SAMs due to the densely packed structures.

**Photoelectrochemistry of $C_{60}$ SAM Systems.** Photoelectrochemical measurements were carried out for **1**/Au in an argon-saturated 0.1 M $Na_2SO_4$ solution containing 50 mM ascorbic acid (AsA) as an electron sacrificer using the modified gold electrode as a working electrode, a platinum counter

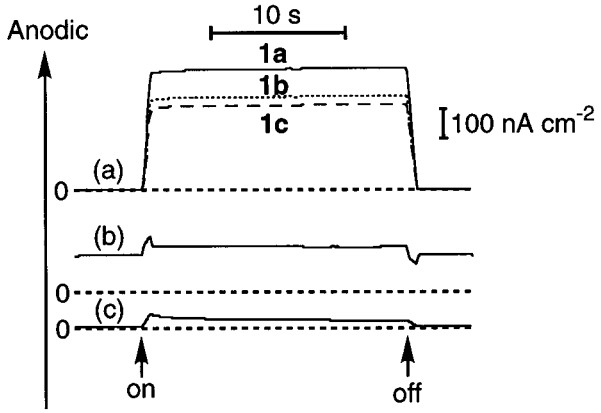


**Figure 4.** Photoelectrochemical response of (a) Au/**1a**/AsA/Pt cell (solid line), Au/**1b**/AsA/Pt cell (dotted line), Au/**1c**/AsA/Pt cell (dashed line), (b) bare Au/AsA/Pt, and (c) Au/**1a**/Pt cell irradiated with $\lambda = 403$ nm light of 6.6 mW cm$^{-2}$ and +0.1 V bias voltage under argon atmosphore. The baseline is shown as a dashed line.

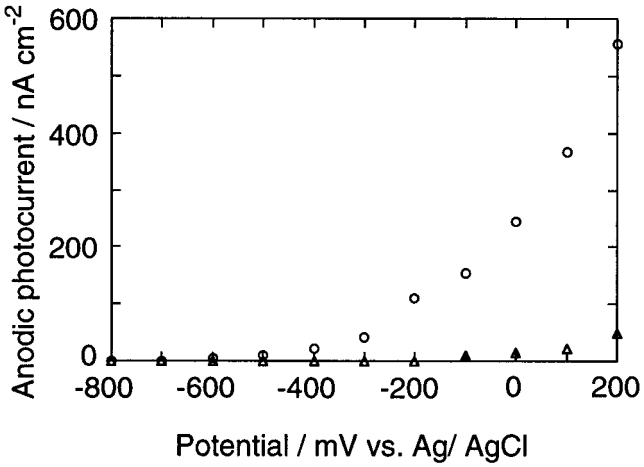


**Figure 5.** Anodic photocurrent vs applied potential curves for Au/**1a**/AsA/Pt cell (circles) and bare Au/AsA/Pt cell (triangles).

electrode, and a Ag/AgCl reference electrode (hereafter, Au/**1**/AsA/Pt, where / represents an interface). A stable anodic photocurrent from the electrolyte to the gold electrode appeared immediately after the irradiation of the gold electrode with $\lambda = 403 \pm 6.9$ nm light of 6.6 mW cm$^{-2}$ and +0.1 V bias voltage, as shown in Figure 4. The photocurrent fell down instantly when the illumination was terminated. The photoelectrochemical response was repeated for tens of times without any signs of attenuation. The intensity of the photocurrent was maintained substantially during the irradiation of at least 2 h. There is a good linear relationship between the intensities of the photocurrent and the light (from 0.25 to 6.6 mW cm$^{-2}$). The photocurrent increases linearly with an increase of the concentration of AsA at low concentration (<1 mM), then deviates gradually from the slope, and eventually becomes constant at around 50 mM (the half saturation value of the AsA: 20 mM). The intensities of the photocurrent for the Au/**1**/AsA/Pt cell increase gradually in the order of **1c**, **1b**, and **1a**. These are an order of magnitude larger than those of the bare Au/AsA/Pt cell or the Au/**1**/Pt cell, indicating the involvement of $C_{60}$ and AsA for the photocurrent generation (Figure 4). The anodic photocurrent increases with an increase of positive bias to the gold electrode (−800 mV to +200 mV) in the Au/**1a**/AsA/Pt cell, whereas a slight increase of the photocurrent was observed in the bare gold electrode system (Figure 5). This demonstrates that the photocurrent flows from the electrolyte to the gold

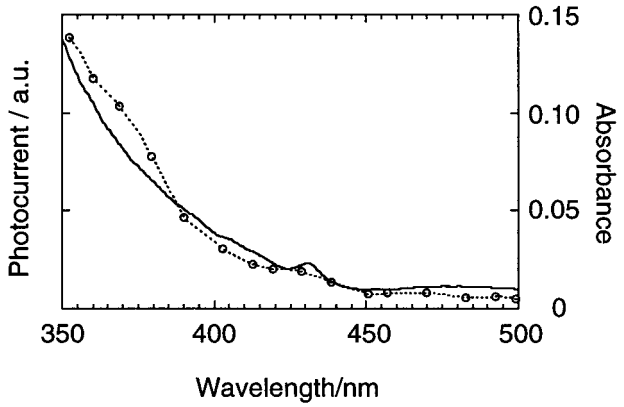


**Figure 6.** Action spectrum of Au/**1a**/AsA/Pt cell (dotted line with circles) and absorption spectrum of **1a** in $CHCl_3$ (solid line, 8.88 × 10$^{-6}$ M).

electrode via the excited states of $C_{60}$. However, a further increase of positive bias to the gold electrode (>+200 mV) could not be carried out, because of significant increase of the anodic current as the dark current. The intensity of the photocurrent dramatically increased as the potential was applied more positive around −600 mV, which is good agreement with the redox potential of the $C_{60}$. This indicates that the photocurrent generation is controlled by the electron transfer rate between the gold electrode and the $C_{60}$. The agreement of the action spectrum (input power: 1 mW cm$^{-2}$ at each wavelength) with the absorption spectrum of **1a** in $CHCl_3$ in the range of 350−500 nm (Figure 6) shows that the $C_{60}$ is responsible for the photocurrent generation. Similar photoelectrochemical behavior was observed for Au/**1b**/AsA/Pt and Au/**1c**/AsA/Pt cells. Under the excitation with $\lambda = 403 \pm 6.9$ nm light of 6.6 mW cm$^{-2}$ and +0.1 V bias voltage, we obtained a photocurrent density of 380 nA cm$^{-2}$ for the Au/**1a**/AsA/Pt cell. Assuming that the absorption coefficient of **1a** on gold surface is the same as that in $CHCl_3$ ($\epsilon = 4.11 \times 10^3$ M$^{-1}$ cm$^{-1}$ at 403 nm), absorbance of **1a**/Au including the reflection at 403 nm is calculated to be $7.81 \times 10^{-4}$. Given the absorbance for **1a**/Au, we can estimate that the quantum yield of Au/**1a**/AsA/Pt cell is 9.8%. Similarly, the values for the Au/**1b**/AsA/Pt and Au/**1c**/AsA/Pt cells are calculated to be 8.6% and 7.5%, respectively (Table 1).

## Discussion

Cyclic voltammetry of **1** in solution and **1**/Au as well as the blocking experiments using the redox probe have established the structure of the fullerene thin films. These results support the well-packed structures of $C_{60}$ moieties on gold electrodes. The packing densities ($1.3-1.4 \times 10^{-10}$ mol cm$^{-2}$) were slightly lower than that calculated for compact monolayers of $C_{60}$, assuming fcc packing and an area of 100 Å$^2$ molecule$^{-1}$ ($1.9 \times 10^{-10}$ mol cm$^{-2}$).[9] Hussey et al. reported that interchain hydrogen bonding enhances the stability of the monolayers but reduces the packing densities.[17] The slight decrease in the packing density may be related to this effect, in addition to the steric hindrance around the phenyl spacer on the $C_{60}$. From the electrochemical studies, there is no significant difference among the three types of the modified gold electrodes. Although these results support that the structures of the alkanethiol monolayers underlying the $C_{60}$ moieties do not change substantially depending on the substitution positions, the packing structures of the $C_{60}$ moieties overlying the alkanethiols may be different among the three isomers. Therefore, we can examine the dependence

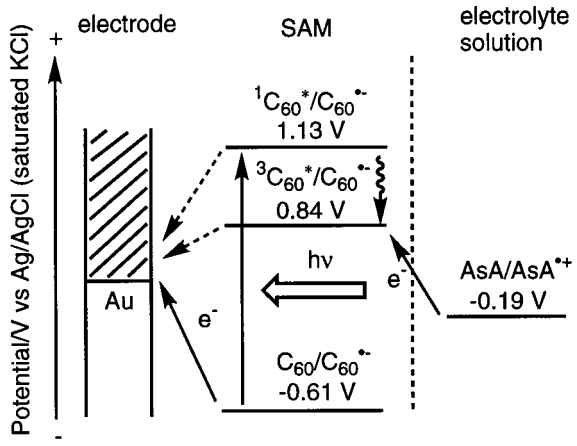


**Figure 7.** Photocurrent generation mechanism in Au/**1**/AsA/Pt cell. Deactivation pathway of the excited states of the $C_{60}$ by the gold electrode is shown as dashed arrow.

of the photoelectrochemical properties on the substitution positions of the $C_{60}$ chromophores, as we will discuss later.

The quantum yields of the $C_{60}$ cells are at least one order of magnitude larger than those in similar photoelectrochemical cells of porphyrin SAMs[27,28] and comparable to those (1.2−8.2%) in similar $C_{60}$ LB cells[29,30] and lipid bilayer cells (4−6%) using $C_{60}$ and $C_{70}$.[31−33] The highest value (9.8%) is also comparable to the previously reported highest value (11%)[34] among the photoelectrochemical cells mimicking photosynthetic electron transfer.[35−43] These results show that $C_{60}$ is an excellent electron mediator as well as a good electron acceptor, owing to the small reorganization energy in electron transfer, as we reported previously.[44,45]

On the basis of the data together with the previous results, we can propose the photocurrent generation mechanism as illustrated in Figure 7. It is known that the triplet states of $C_{60}$ and its derivatives are produced with a almost unity yield (0.85−1) via intersystem crossing from the excited singlet state. It is possible energetically that both the excited singlet state (1.13 V vs Ag/AgCl) and the triplet state (0.84 V) of the $C_{60}$ are quenched by AsA (−0.19 V, pH 7.0). The lifetimes of the singlet and triplet states of the monofunctionalized $C_{60}$ are reported to be 1.2−1.4 ns and 20−140 $\mu$s, respectively.[45] The electron transfer rate from AsA to the excited states of the $C_{60}$ is controlled by diffusion of AsA in the electrolyte solution. Since the anodic photocurrent is saturated at <50 mM AsA, it is only the triplet state of the $C_{60}$ that is reacting with AsA. In fact, given the half saturation concentration of AsA (20 mM) and the encounter limited rate constant ($5 \times 10^9$ $M^{-1}$ $s^{-1}$), the lifetime of the triplet state is calculated to be 10 ns. The resulting $C_{60}$ anion radical would give an electron to the gold electrode, leading to the recovery of the initial state. Totally, the vectorial anodic electron flow occurs from AsA to the gold electrode via the excited triplet state of the $C_{60}$.

It is interesting to compare the quantum yields among the three $C_{60}$ cells. The quantum yield increases slightly in the order of ortho, meta, and para depending on the linking position of the substituted phenyl ring. Creager et al. reported the bridge-mediated long-range electronic coupling between ferrocene and gold in alkanethiolate-based monolayers on gold electrodes.[46] They concluded that a donor−acceptor linked system and an electrode−donor (or acceptor) linked system are similar from the viewpoint of long-range electronic coupling in electron transfer. It is well established that the through-bond electronic coupling at the meta position is much weaker than those at para and ortho positions when a donor is linked to an acceptor via a spacer involving a phenyl ring.[47] Assuming the electronic coupling trend in electron transfer, the electron transfer rate between the gold electrode and the $C_{60}$ with meta linkage may be much slower than those with para and ortho linkage. Thus, the intensity of the photocurrent in the Au/**1b**/AsA/Pt cell would be much reduced compared with those in the Au/**1a**/AsA/Pt and Au/**1c**/AsA/Pt cells. However, the tendency was not observed in the Au/**1a**, **1b**, and **1c**/AsA/Pt cells. Ascorbic acid is an electron sacrificer and the cation radical produced via electron transfer is decomposed immediately. Accordingly, the lifetime of $C_{60}^{\bullet-}$ generated by AsA is much prolonged because of the inhibition of charge recombination. In addition, the charge shift from the $C_{60}^{\bullet-}$ to the gold electrode may be accelerated, whereas the charge recombination is retarded because of the small reorganization energy of $C_{60}$, as we proposed previously.[44,45,47] The long lifetime of $C_{60}^{\bullet-}$ would make it possible to shift an electron from $C_{60}^{\bullet-}$ to the gold efficiently. Therefore, even if there is a difference of the rate constant for the charge shift among the three isomers, the effect would be masked so that the intensities of the photocurrent as final output do not vary much. It is well known that the excited states of dyes on metal surface are quenched efficiently by the metal via energy transfer.[48−50] We have already reported porphyrin SAM systems where the porphyrins are assembled on the gold electrodes with different spacer lengths. The excited states of the porphyrins are quenched much more strongly by the gold electrodes as the spacer lengths decrease. The preliminary fluorescence studies on the $C_{60}$ SAM system on gold electrodes were unsuccessful because of the weak fluorescence from the $C_{60}$. However, we believe that the relatively long spacer in **1** would prevent the excited states of the $C_{60}$ significantly from quenching by the gold electrode via energy transfer. Considering that the surface coverages are quite similar among the three systems, the slight difference of the photocurrents might be related to the quenching rates between the gold electrode and the excited states of the $C_{60}$ and/or the self-quenching of the aggregated $C_{60}$ moieties in the excited states due to the difference of the linkage.

In conclusion, photoelectrochemical cells with gold electrodes modified with $C_{60}$ SAMs have been constructed systematically. The high quantum yields imply that $C_{60}$ SAMs are promising for applications in materials science. Our results provide basic information for the development of photovoltaic devices and sensors as well as electron transfer in molecular assemblies.

**Acknowledgment.** This work was supported by Grant-in-Aids for COE Research and Scientific Research on Priority Area of Electrochemistry of Ordered Interfaces and Creation of Delocalized Electronic Systems from Ministry of Education, Science, Sports and Culture, Japan. Y.S. thanks the Mitsubishi Foundation for financial support.

**Supporting Information Available:** The synthesis and characterization of $C_{60}$ alkanethiols. This material is available free of charge via the Internet at http://pubs.acs.org.

## References and Notes

(1) Dresselhaus, M. S.; Dresselhaus, G.; Eklund, P. C. *Science of Fullerenes and Carbon Nanotubes*; Academic Press: San Diego, 1996.

(2) Mirkin, C. A.; Caldwell, W. B. *Tetrahedron* **1996**, *52*, 5113.

(3) Ulman, A. *Introduction to Ultrathin Organic Films*; Academic Press: San Diego, 1991.

(4) Chen, K.; Caldwell, W. B.; Mirkin, C. A. *J. Am. Chem. Soc.* **1993**, *115*, 1193.

(5) Chupa, J. A.; Xu, S.; Fischetti, R. F.; Strongin, R. M.; McCauley, J. P., Jr.; Smith, A. B., III; Blasie, J. K.; Peticolas, L. J.; Bean, J. C. *J. Am. Chem. Soc.* **1993**, *115*, 4383.

(6) Caldwell, W. B.; Chen, K.; Mirkin, C. A.; Babinec, S. J. *Langmuir* **1993**, *9*, 1945.
(7) Tsukruk, V. V.; Lander, L. M.; Brittain, W. J. *Langmuir* **1994**, *10*, 996.
(8) Shi, X.; Caldwell, W. B.; Chen, K.; Mirkin, C. A. *J. Am. Chem. Soc.* **1994**, *116*, 11598.
(9) Arias, F.; Godínez, L. A.; Wilson, S. R.; Kaifer, A. E.; Echegoyen, L. *J. Am. Chem. Soc.* **1996**, *118*, 6086.
(10) Domínguez, O.; Echegoyen, L.; Cunha, F.; Tao, N. *Langmuir* **1998**, *14*, 821.
(11) Kim, S. H.; Lee, S. H.; Kang, S. H. *Tetrahedron Lett.* **1998**, *39*, 9693.
(12) Imahori, H.; Azuma, T.; Ozawa, S.; Yamada, H.; Ushida, K.; Ajavakom, A.; Norieda, H.; Sakata, Y. *Chem. Commun.* **1999**, 557.
(13) Lenk, T. J.; Hallmark, V. M.; Hoffmann, C. L.; Rabolt, J. F.; Castner, D. G.; Erdelen, C.; Ringsdorf, H. *Langmuir* **1994**, *10*, 4610.
(14) Tam-Chang, S.-W.; Biebuyck, H. A.; Whitesides, G. M.; Jeon, N.; Nuzzo, R. A. *Langmuir* **1995**, *11*, 4371.
(15) Clegg, R. S.; Hutchison, J. E. *Langmuir* **1996**, *12*, 5239.
(16) Yu, H. Z.; Shao, H. B.; Luo, Y.; Zhang, H. L.; Liu, Z. F. *Langmuir* **1997**, *13*, 5774.
(17) Sabapathy, R. C.; Bhattacharyya, S.; Leavy, M. C.; Cleland, W. E., Jr.; Hussey, C. L. *Langmuir* **1998**, *14*, 124.
(18) Suzuki, T.; Li, Q.; Khemani, K. C.; Wudl, F.; Almarsson, Ö. *Science* **1991**, *254*, 1186.
(19) Suzuki, T.; Li, Q.; Khemani, K. C.; Wudl, F.; Almarsson, Ö. *J. Am. Chem. Soc.* **1992**, *114*, 7300.
(20) Prato, M.; Suzuki, T.; Foroudian, H.; Li, Q.; Khemani, K.; Wudl, F.; Leonetti, J.; Little, R. D.; White, T.; Rickborn, B.; Yamago, S.; Nakamura, E. *J. Am. Chem. Soc.* **1993**, *115*, 1594.
(21) Arias, F.; Xie, Q.; Wu, Y.; Lu, Q.; Wilson, S. R.; Echegoyen, L. *J. Am. Chem. Soc.* **1994**, *116*, 6388.
(22) Boudon, C.; Gisselbrecht, J.-P.; Gross, M.; Isaacs, L.; Anderson, H. L.; Faust, R.; Diederich, F. *Helv. Chim. Acta* **1995**, *78*, 1334.
(23) Tomioka, Y.; Ishibashi, M.; Kajiyama, H.; Taniguchi, Y. *Langmuir* **1993**, *9*, 32.
(24) Matsumoto, M.; Tachibana, H.; Azumi, R.; Tanaka, M.; Nakamura, T.; Yunome, G.; Abe, M.; Yamago, S.; Nakamura, E. *Langmuir* **1995**, *11*, 660.
(25) Nakanishi, T.; Murakami, H.; Nakashima, N. *Chem. Lett.* **1998**, 1219.
(26) Porter, M. D.; Bright, T. B.; Allara, D. L.; Chidsey, C. E. D. *J. Am. Chem. Soc.* **1987**, *109*, 3559.
(27) Akiyama, T.; Imahori, H.; Sakata, Y. *Chem. Lett.* **1994**, 1447.
(28) Imahori, H.; Norieda, H.; Ozawa, S.; Ushida, K.; Yamada, H.; Azuma, T.; Tamaki, K.; Sakata, Y. *Langmuir* **1998**, *14*, 5335.
(29) Luo, C.; Huang, C.; Gan, L.; Zhou, D.; Xia, W.; Zhuang, Q.; Zhao, Y.; Huang, Y. *J. Phys. Chem.* **1996**, *100*, 16685.
(30) Luo, C.; Gan, L.; Zhou, D.; Huang, C. *J. Chem. Soc., Faraday Trans.* **1997**, *93*, 3115.
(31) Hwang, K. C.; Mauzerall, D. *J. Am. Chem. Soc.* **1992**, *114*, 9705.
(32) Hwang, K. C.; Mauzerall, D. *Nature* **1993**, *361*, 138.
(33) Niu, S.; Mauzerall, D. *J. Am. Chem. Soc.* **1996**, *118*, 5791.
(34) Uosaki, K.; Kondo, T.; Zhang, X.-Q.; Yanagida, M. *J. Am. Chem. Soc.* **1997**, *119*, 8367.
(35) Seta, P.; Bienvenue, E.; Moore, A. L.; Mathis, P.; Bensasson, R. V.; Liddell, P. A.; Pessiki, P. J.; Joy, A.; Moore, T. A.; Gust, D. *Nature* **1985**, *316*, 653.
(36) Fujihira, M.; Nishiyama, K.; Yamada, H. *Thin Solid Films* **1985**, *132*, 77.
(37) Sakata, Y.; Tatemitsu, H.; Bienvenue, E.; Seta, P. *Chem. Lett.* **1988**, 1625.
(38) Akiyama, T.; Imahori, H.; Ajavakom, A.; Sakata, Y. *Chem. Lett.* **1996**, 907.
(39) Steinberg-Yfrach, G.; Liddell, P. A.; Hung, S.-C.; Moore, A. L.; Gust, D.; Moore, T. A. *Nature* **1997**, *385*, 239.
(40) Kondo, T.; Yanagida, M.; Nomura, S.-I.; Ito, T.; Uosaki, K. *J. Electroanal. Chem.* **1997**, *438*, 121.
(41) Steinberg-Yfrach, G.; Rigaud, J.-L.; Durantini, E. N.; Moore, A. L.; Gust, D.; Moore, T. A. *Nature* **1998**, *392*, 479.
(42) Aoki, A.; Abe, Y.; Miyashita, T. *Langmuir* **1999**, *15*, 1463.
(43) Imahori, H.; Ozawa, S.; Ushida, K.; Takahashi, M.; Azuma, T.; Ajavakom, A.; Akiyama, T.; Hasegawa, M.; Taniguchi, S.; Okada, T.; Sakata, Y. *Bull. Chem. Soc. Jpan.* **1999**, *72*, 485.
(44) Imahori, H.; Hagiwara, K.; Akiyama, T.; Aoki, M.; Taniguchi, S.; Okada, T.; Shirakawa, M.; Sakata, Y. *Chem. Phys. Lett.* **1996**, *263*, 545.
(45) Imahori, H.; Sakata, Y. *Adv. Mater.* **1997**, *9*, 537.
(46) Weber, K.; Hockett, L.; Creager, S. *J. Phys. Chem. B* **1997**, *101*, 8286.
(47) Imahori, H.; Hagiwara, K.; Aoki, M.; Akiyama, T.; Taniguchi, S.; Okada, T.; Shirakawa, M.; Sakata, Y. *J. Am. Chem. Soc.* **1996**, *118*, 11771.
(48) Waldeck, D. H.; Alivisatos, A. P.; Harris, C. B. *Surf. Sci.* **1985**, *158*, 103.
(49) Zhou, X.-L.; Zhu, X.-Y.; White, J. M. *Acc. Chem. Res.* **1990**, *23*, 327.
(50) Barnes, W. L. *J. Mod. Opt.* **1998**, *45*, 661.